Correlation between strain and excess carrier lifetime in a 3C-SiC wafer

Atsushi Yoshida[1,a], Masashi Kato[1,b], Masaya Ichimura[1,c]

[1] Graduate School of Engineering, Nagoya Institute of Technology, Gokiso, Showa, Nagoya, 466-8555 Japan

{[a]ciq16607@stn., [b]kato.masashi@, [c]ichimura.masaya@}nitech.ac.jp

Keywords: 3C-SiC, carrier lifetime, strain, μ-PCD method

Abstract. We obtained excess carrier lifetime maps by the microwave photoconductivity decay (μ-PCD) method in a free-standing n-type 3C-SiC wafer, and then we compared the lifetime maps with distributions of strains and defects observed by the optical microscopy and the Raman spectroscopy. We found that the excess carrier lifetimes are short in a strained region in 3C-SiC, which indicates that structural defects exist around a strained region.

Intorduction

3C-SiC is a promising material for low loss and high voltage power devices. Compared with 4H- and 6H-SiC, 3C-SiC devices are expected to show high electron mobility owing to high quality metal-oxide-semiconductor (MOS) interface. In addition, electric breakdown field of 3C-SiC MOS field effect transistor (FET) has been reported to reach 8.5 MV/cm which is close to values of 4H- and 6H-SiC MOSFET [1]. However, 3C-SiC devices have never been commercialized because of presence of defects and strains due to lattice mismatch between Si and 3C-SiC since 3C-SiC is usually grown epitaxially on Si substrates. Therefore, effects of defects and strains on electrical characteristics should be elucidated. Although some studies of carrier lifetime in 3C-SiC wafers have been reported so far [2-4], correlation between distribution of defects and carrier lifetimes is not clarified. In this work, we evaluate excess carrier lifetime by the microwave photoconductivity decay (μ-PCD) method, and then we compare the lifetime maps with distributions of strains and defects.

Experiments

The sample was a free-standing n-type 3C-SiC wafer. It was epitaxially grown on an undulant Si (100) substrate. A photograph of the sample is shown in Fig. 1. As can be seen in this figure, there are stripes in the sample in the horizontal direction. We defined the grown surface as the epi-side, the substrate-side surface as the sub-side. In the μ-PCD method, we used a 355 nm pulsed YAG laser (the penetration depth is 4.7 μm, and the spot diameter is 200 μm) as an excitation source, and microwave of 10 GHz as a probe. In the measurements, we used rectangular waveguides in which the TE_{10} mode is basic mode of the microwave conduction. When the stripes of the sample are parallel to the electric field in the μ-PCD measurements, we call the configuration "parallel". When the strips are vertical to the electric field, we call the configuration "vertical". From excess carrier decay curves obtained by μ-PCD, we mapped 1/e lifetime, which is defined as time interval of the excess carrier decay from a peak to 1/e. The strain fields were observed by the microscope with crossed polarizers. Defects around a strained region were characterized by the micro Raman spectroscopy and observation after molten NaOH etching, and crystalline quality of the sample was evaluated by X-ray diffraction.

Results and discussion

Optical micrograph of the samples with crossed polarizers is shown in Fig. 2. Contrast due to strains is observed at the lower half of the middle in this figure. Profiles of the sub- and epi-sides obtained by a laser microscopy along the X-axis in Fig. 2 are shown in Figs. 3 and 4, respectively. A depression is

observed in Fig.3, and this depression seems to be located at the strained region in Fig.2. In contrast, the epi-side is fairly flat as shown in Fig. 4.

The carrier lifetime map for the sub-side measured with the vertical configuration is shown in Fig. 5. We found a region with short 1/e lifetimes elongated parallel to the Y axis at X = 500-800 μm. Points A, B and C in this figure correspond to the points in Fig. 2 and the excess carrier decay curves for these points are shown in Fig. 6. These decay curves show initial fast decay components followed by slow decay components, and a time constant for initial decay at point B, which corresponds to the strained region, is smaller than those for points A and C.

The carrier lifetime map for the epi-side measured with the vertical configuration is shown in Fig. 7. The mapped regions are slightly different from Fig. 5, and the axes are scaled so that the coordinates in Figs. 5 and 7 correspond. We found a region with short 1/e lifetimes elongated parallel to the Y axis at X=600-900 μm similarly to Fig. 5. Thus carrier lifetimes in the strained region are short in measurements on both the sides, although, as shown in Figs. 2 and 3, the strained region is depressed on the sub-side but is flat on the epi-side. Therefore, we did not find correspondence between 1/e lifetimes and roughness of the surface.

1/e lifetimes obtained from the epi-side are longer than obtained from the sub-side at most of the regions. In the X-ray rocking curve, the full width at half maximum (FWHM) of the 3C-SiC (200) peak for the epi- and sub-sides are 0.064° and 0.040°, respectively. Generally, the carrier lifetime is long in a high-quality single crystal with small FWHM in the rocking curve, but 1/e lifetimes for the epi-side are larger than those for the sub-side. Therefore, the 1/e lifetime difference between the epi- and sub-sides does not have general relationship to the crystallinity observed by X-ray diffraction.

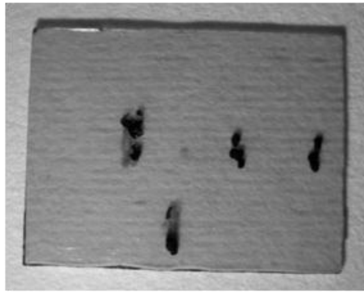

Fig. 1: Sample photograph. Black dots are markings for microscopic measurements.

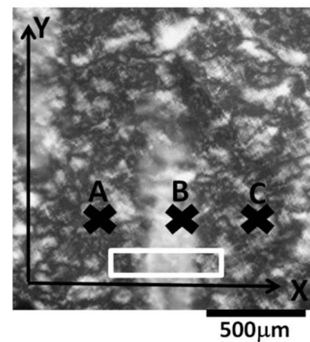

Fig. 2: Optical micrograph with crossed polarizers.

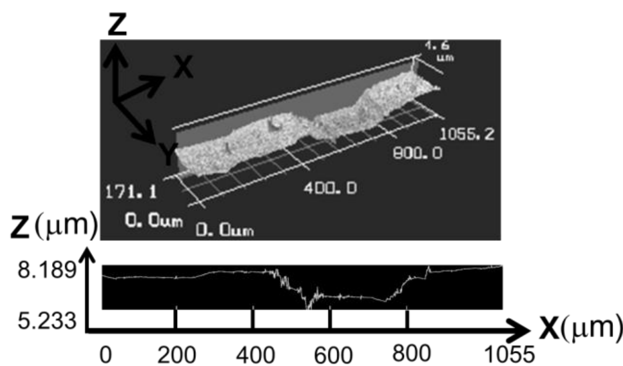

Fig. 3: profile of the sub-side along the X axis of Fig.2.

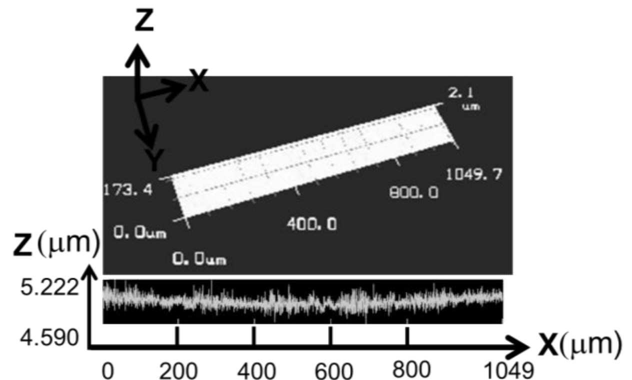

Fig. 4: profile of the epi-side along the X axis of Fig.2.

After mechanical polishing on the sub-side to remove the depression, the sample was etched by molten NaOH at 550 °C for 10 min. The optical micrographs for the sub- and epi-sides after the etching are shown in Figs. 8 (a) and (b) along with the micrograph with crossed polarizers (Fig. 8(c)), and these micrographs are for the same region of the sample. In Fig. 8 (a), irregular shape pits are observed, while line pits are observed in Fig. 8 (b). We consider that the line pits on the epi-side

indicate presence of stacking fault (SF), and their densities seem to be high on the strained region by comparing Figs 8 (b) with (c). This result suggests that the strain regions have high density of SF.

The Raman spectra of inside and outside of the strain regions are shown in Fig. 9. A peak of the TO phonon is observed at 790 cm^{-1}. Because the TO phonon is a forbidden mode for the 3C-SiC (001) orientation in the backscattering arrangement, we consider that the TO peak intensity is related to defect density. The maps of TO/LO peak intensity ratios in the area surrounded by the white line in Fig. 2 are shown in the inset of Fig. 9. The TO intensity becomes larger in the strained region, and thus defect density wound be high in the strained region as observed by etch pits in Fig 8 (b). This result suggests that carrier lifetime decreases due to presence of the defects in the strained region in the 3C-SiC wafer.

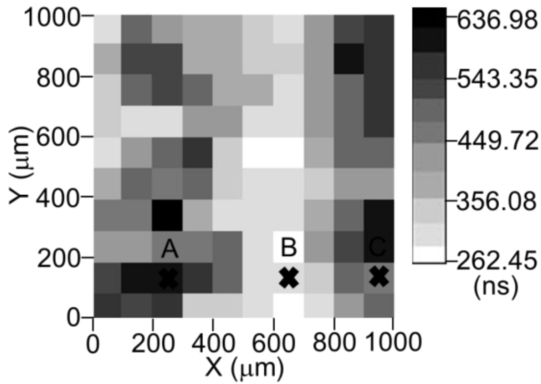

Fig. 5: Carrier lifetime maps for the sub-side with the vertical configurration.

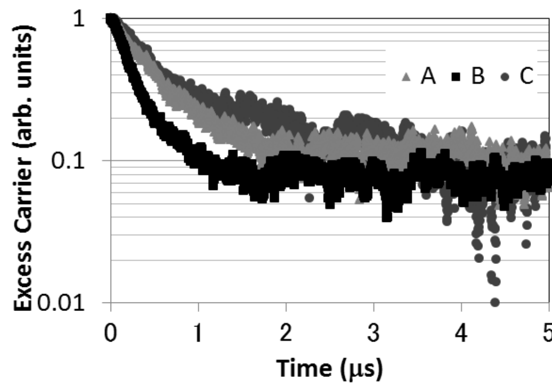

Fig. 6: Excess carrier decay curves for points A, B and C in Fig. 5.

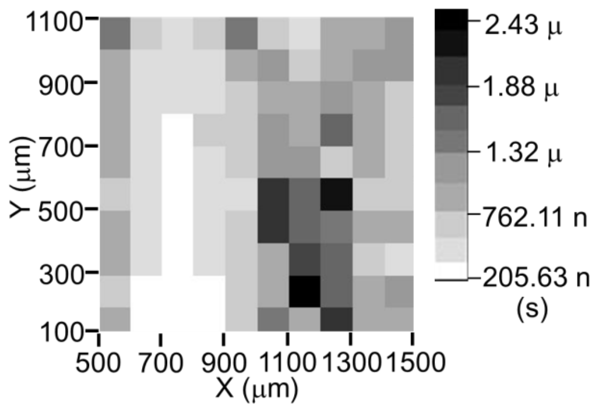

Fig. 7: Carrier lifetime maps for the epi-side with the vertical configurration.

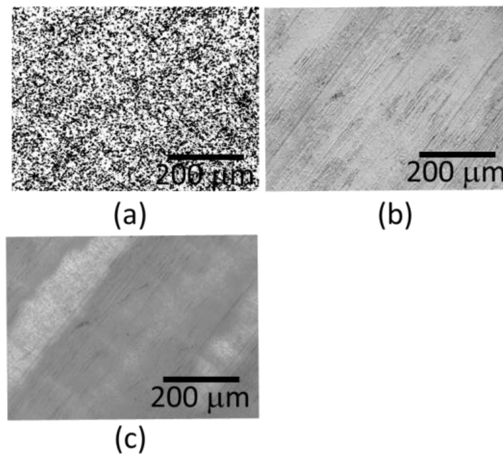

Fig. 8: Optical micrographs after NaOH etching for (a) the sub-side, (b) the epi-side And (c) observed with crossed polarizers.

A carrier lifetime map for the sub-side measured with the parallel configuration is shown in Fig. 10. Because the sample was rotated by 90°, the X- and Y- axis are also rotated from Figs. 5 and 7. In this figure, we did not find a region with short 1/e lifetimes. On the other hand, we were not able to obtain a carrier lifetime map for the epi-side with the parallel configuration because of weak μ-PCD signals. Thus μ-PCD signals measured with the parallel configuration are different from those measured with the vertical configuration. Movement directions of excited carriers should depend on directions of microwave electric field and should be different between measurements with the parallel and vertical configurations. It has been reported that Hall mobility is larger in the direction parallel to SF than in the direction vertical to SF in 3C-SiC grown on undulant Si [5], and thus a carrier scattering mechanism in such 3C-SiC is anisotropic. We can expect that carrier recombination mechanisms in

our 3C-SiC are also anisotropic, and carrier lifetime map depends on configuration of the sample in the μ-PCD measurements. However, we need further investigation for this configuration dependence of the carrier lifetime.

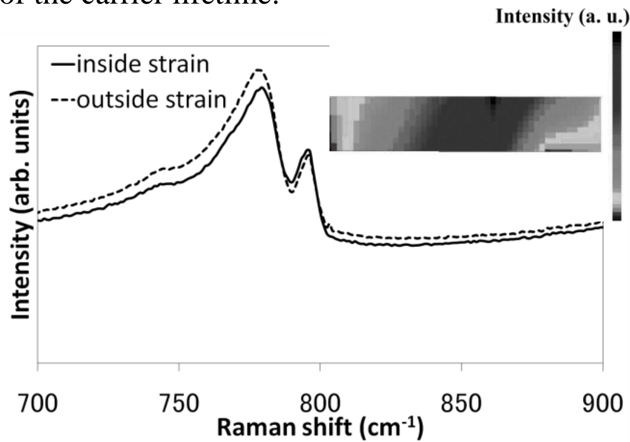

Fig. 9: Raman spectra of inside and outside of strain fields. The inset is a Raman map for the TO/LO peak intensity ratio in the area surrounded by the white line in Fig. 2.

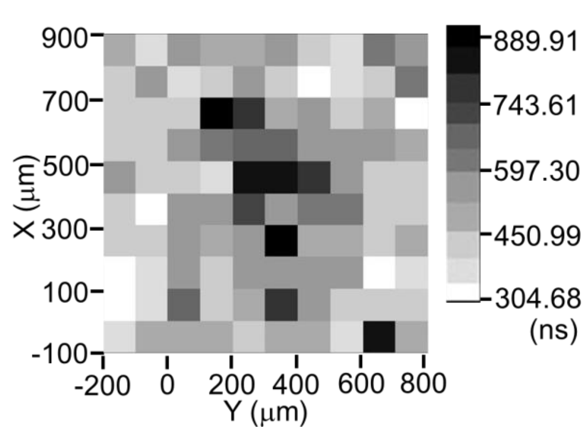

Fig. 10: Carrier lifetime maps for the sub-side with the parallel configurration.

Conclusions

We mapped the carrier lifetime in 3C-SiC epitaxially grown on an undulant Si (100) substrate by the μ-PCD method. We found that the carrier lifetime is short in the strained region but does not depend on the crystallinity observed by X-ray diffraction. From the Raman spectroscopy results and the pit concentration after etching, we also found that the defects exsit with high concentration in the strained region. These results suggest that the carrier lifetimes decrease in the region with strain and defects.

Acknowledgment

We would like to thank Prof. K. Jarasiunas and Mr. P. Scajev of Vilinius University for their fruitful discussion.

References

[1] T. Ohshima, K. K. Lee, Y. Ishida, K. Kojima, Y. Tanaka, T. Takahashi, M. Yoshikawa, H. Okumura, K. Arai and T. Kamiya, Jpn. J. Appl. Phys. Vol. 42 (2003) p.L625.

[2] V. Grivackas, G. Manolis, K. Gulbinas, K. Jarašiūnas, M. Kato, Appl. Phys. Lett. Vol.95 (2009) 242110.

[3] M. Ichimura, N. Yamada, H. Tajiri, and E. Arai, J. Appl. Phys. Vol.84 (1998) p.2727.

[4] P. Ščajev, J. Hassan, K. Jarašiūnas, M. Kato, A. Henry, and J. P. Bergman, J. Electron. Mater. Vol.40 (2010) p.394.

[5] H. Nagasawa, K. Yagi, T. Kawahara, N. Hatta, G. Pensl, W. J. Choyke, T. Yamada, K. M. Itoh and A. Schöner: W. J. Choyke, H. Matsunami, G. Pensl (Eds.), Springer-Verlag, Berlin, Heidelberg (2004) p.207.